

Variation Based Extended Kalman Filter on S^2

Prasanth Kotaru and Koushil Sreenath

Abstract—In this paper, we propose a variation-based extended Kalman filter (V-EKF) on the two-sphere manifold. We consider the spherical pendulum dynamical system whose nonlinear geometric dynamics evolve on the two-sphere. These dynamics are linearized about the current state using a variation-based linearization resulting in a time-varying linear system with state constraints that describe the dynamics of the variation states. The Kalman filter is applied on the resulting variation states with the pendulum position as measurements for measurement updates. The V-EKF also has a *constraint* update where the estimated state and covariance are updated to ensure they satisfy the constraints. Desirable properties of V-EKF, such as preserving the geometric structure of the estimated state are thus achieved. The proposed method is illustrated through numerical simulations and also validated through experiments.

I. INTRODUCTION

The set of all points in the Euclidean space \mathbb{R}^3 , that lie on the surface of the unit ball about the origin belong to the two-sphere manifold, S^2 . It is a two-dimensional manifold that is locally diffeomorphic to \mathbb{R}^2 . Many mechanical systems such as a spherical pendulum, double pendulum, quadrotor with a cable-suspended load, evolve on either S^2 or products comprising of S^2 . Typically, systems that evolve on S^2 are parametrized by azimuthal angles (spherical coordinates) with respect to a local reference system. Prior estimation algorithms on S^2 use the local parameterizations and estimate the azimuthal angles. However such estimators are not valid globally and have singularities. Our work addresses this by directly estimating the states on TS^2 , the tangent bundle of S^2 , and is thus free of singularities.

In recent times, many robotic systems with configuration spaces that include two-sphere manifolds are studied for various applications. For instance, dynamics for multiple quadrotors with payload suspended from cables, [12], [13], [8], [2] or three-link walkers [1] are defined with cable/link attitude represented using the two-sphere, S^2 . Due to the coordinate-free nature of these dynamics, controllers that exhibit almost global stability properties [12], [4] can be designed. Most controllers assume complete and accurate knowledge of the state and thus require the best state estimate, like link attitude and angular velocity, to achieve the desirable results.

Kalman filters for nonlinear systems such as extended Kalman filter (EKF) and unscented Kalman filter (UKF) can be used for estimation on the two-sphere S^2 . However, the measurement update of these Kalman filters is performed

P. Kotaru and K. Sreenath are with the Dept. of Mechanical Engineering, University of California, Berkeley, CA, 94720 {prasanth.kotaru, koushils}@berkeley.edu.

This work was supported in part by NSF grant CMMI-1840219.

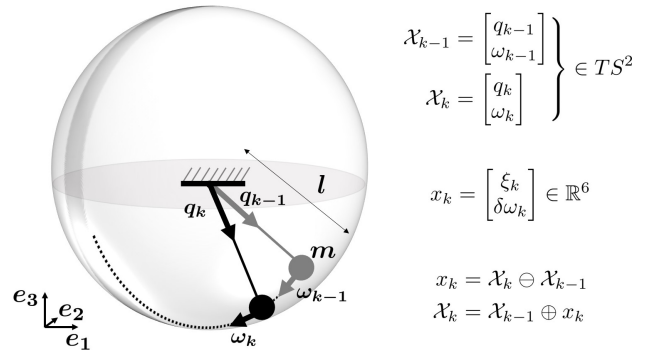


Fig. 1: The Spherical Pendulum model evolves on S^2 with the attitude of the pendulum represented by a unit-vector $q \in S^2$. Angular velocity of the pendulum at a point q in S^2 is in the tangent space $T_q S^2 = \{\omega \in \mathbb{R}^3 \mid \omega \cdot q = 0\}$.

in the Euclidean space and thus, the estimated state is not guaranteed to lie on S^2 . Thus, estimators that estimate directly on the manifold are required. One such estimator, a set-bounded estimator for the spherical pendulum that uses a global, coordinate-free parametrization is developed in [6]. In the set-bounded estimator, the pendulum attitude is represented $SO(3)$ with a symmetry axis, effectively reducing the attitude to S^2 and assumes bounded measurement noise. Unlike, the set-bounded estimators our work provides global formulation of an EKF for S^2 estimation using variation based methods, similar to estimation of states on $SE(3)$ in [5].

The goal of our work is to estimate the state of the spherical pendulum $X_k \in TS^2$ at time $t = t_k$, given noisy estimate of the pendulum state X_{k-1} at time $t = t_{k-1}$ and measurements of the Cartesian position $z_k \in \mathbb{R}^3$ of the pendulum's bob with respect to the suspension point. Our approach is to formulate a variation-based extended Kalman filter that (a) propagates the continuous-time dynamics on TS^2 using a variational-based integrator to construct the *a priori* pendulum state estimate, (b) derives the geometric variation-based linearization of the nonlinear dynamics and formulates the geometric variation $x_k \in \mathbb{R}^6$ between consecutive pendulum states X_k and X_{k-1} , (c) uses the discrete measurements z_k to obtain *a posteriori* estimates of the variation states x_k and its covariance, (d) corrects the *a posteriori* variation state and covariance estimates to enforce the state constraints, and finally (e) constructs the *a posteriori* pendulum state estimate using the variation states.

The main contributions of this work are enumerated below,

- 1) V-EKF is developed for the coordinate-free nonlinear

dynamic model of a spherical pendulum on S^2 and thus, is not subjected to the complexities of local parameterization,

- 2) since the estimation is developed on S^2 , the structure of the spherical pendulum states is preserved,
- 3) variation-based linearized dynamics of the spherical pendulum are used during covariance update of the V-EKF,
- 4) procedure to accurately calculate the variation between two spherical pendulum states (q, ω) is shown,
- 5) proposed V-EKF is demonstrated using numerical simulations and experimental results.

Rest of the paper is structured as follows. Spherical pendulum dynamics, variations on its states and variation-based linearized dynamics are given in Section II. Section II also provides the discrete variational dynamics for the spherical pendulum. Section III provides the notation used in the V-EKF, followed by the variation based extended Kalman filter. Section IV validates the proposed V-EKF through numerical simulations and section V provides the experiment results. Finally, Section VI provides the concluding remarks.

II. SPHERICAL PENDULUM

A typical Extended Kalman Filter (EKF) consists of two steps *time* update and *measurement* update. In the *time* update, nonlinear dynamics of the system are integrated to propagate the state estimate through time, while linearized dynamics are used to update the covariance of the estimated state. In the *measurement* update, estimated state and its covariance are corrected based on the sensor measurements.

In this section, we discuss the spherical pendulum dynamics and analyze variations on its states. We linearize the spherical pendulum dynamics using these variations. Finally, we present discrete variational dynamics for the spherical pendulum, so that the structure of the configuration manifold is preserved when integrated.

A. Spherical Pendulum Dynamics

Consider the spherical pendulum model presented in Figure 1. A spherical pendulum comprises of a mass attached to a fixed point through a suspended cable. Mass of the suspended cable is negligible compared to the attached mass and thus, the cable is considered to be mass-less. The spherical pendulum lies in 3D space with two degrees-of-freedom, thus the configuration of the pendulum is in the space of two-sphere S^2 .

We describe the coordinate-free dynamics for the spherical pendulum with pendulum attitude represented by a unit vector in the two-sphere $S^2 := \{q \in \mathbb{R}^3 \mid q \cdot q = 1\}$. The tangent space of the two-sphere at q , given by $T_q S^2 = \{\omega \in \mathbb{R}^3 \mid \omega \cdot q = 0\}$ (see [10]), is a two-dimensional plane tangent to the unit vector q . Let \mathcal{X} represent the *pendulum state* i.e.,

$$\mathcal{X} = \begin{bmatrix} q \\ \omega \end{bmatrix} \in TS^2. \quad (1)$$

The equations of motion for spherical pendulum is given as,

$$\begin{bmatrix} \dot{q} \\ \dot{\omega} \end{bmatrix} =: \dot{\mathcal{X}} = f(\mathcal{X}) := \begin{bmatrix} \omega \times q \\ -\frac{g}{l}(q \times e_3) \end{bmatrix}, \quad (2)$$

where q is the unit vector representing the attitude of the pendulum, ω is the angular velocity of the pendulum, m is the mass of the pendulum mass, l is the length of the pendulum, g is acceleration due to gravity and e_3 is the third-directional unit vector of the inertial frame.

Dynamics in (2) are linearized using variations and the linearized dynamics are used in the Kalman filter in the later sections. In the next section, we define the variations for q , ω .

B. Variation on S^2

For a given trajectory $q(t)$ on S^2 , variation of the state q is considered, such that the perturbed trajectory is also on S^2 . This is achieved by rotating the vector q , so that the unit-length of the vector q is preserved. Variation on S^2 is expressed in terms of a rotation matrix (represented as an exponential map) in [9] as follows,

$$q^\epsilon(t) = \exp[\epsilon \xi^\times] q(t), \quad (3)$$

for a curve $\xi(t) \in \mathbb{R}^3$ satisfying $\xi(t) \cdot q(t) = 0, \forall t$. The cross-map $(\cdot)^\times : \mathbb{R}^3 \rightarrow so(3)$ is defined such that, $u^\times v = u \times v$, for any $u, v \in \mathbb{R}^3$. The corresponding infinitesimal variation for S^2 is given as,

$$\delta q(t) = \left. \frac{d}{d\epsilon} \right|_{\epsilon=0} \exp[\epsilon \xi^\times] q(t) = \xi^\times q(t). \quad (4)$$

The infinitesimal variation could be roughly treated as a linear approximation of the distance between two points on S^2 . Infinitesimal variation of the angular velocity [9] is denoted by $\delta\omega(t)$ in \mathbb{R}^3 satisfying $q(t) \cdot \omega(t) = 0$. For future use, we define the *variation state* as,

$$x = \begin{bmatrix} \xi \\ \delta\omega \end{bmatrix} \in \mathbb{R}^6. \quad (5)$$

The infinitesimal variation ξ in (3) is always orthogonal to q . Taking the time-derivative of the constraint results in,

$$\xi \cdot q \equiv 0 \implies \dot{\xi} q + \xi \dot{q} = 0. \quad (6)$$

Moreover, the angular velocity ω in (1) is always orthogonal to q . Taking the variation of the constraint results in,

$$q \cdot \omega \equiv 0 \implies (\xi^\times q) \cdot \omega + q \cdot \delta\omega = 0. \quad (7)$$

Thus any variation x of the spherical pendulum state \mathcal{X} has to satisfy the constraints (6) and (7).

Having defined the variations for the states, we now consider variations on the dynamics. This would result in linearization of the dynamics as shown in the next section.

C. Variation-based Linearized Dynamics

Taking variation of the spherical pendulum dynamics in (2) about the current state \mathcal{X} yields the following variation dynamics (see [14]),

$$\delta \dot{q} = \delta\omega \times q + \omega \times \delta q, \quad (8)$$

$$\delta \dot{\omega} = \frac{-g}{l} (\delta q \times e_3). \quad (9)$$

Substituting for $\delta q = \xi^\times q$ from (4), we have the following coordinate-free linearized dynamics,

$$\dot{x} = \underbrace{\begin{bmatrix} qq^T \omega^\times & I_{3 \times 3} - qq^T \\ -\frac{g}{l} e_3^\times q^\times & O_{3 \times 3} \end{bmatrix}}_{\triangleq A} x \quad (10)$$

where $I_{3 \times 3}$ and $O_{3 \times 3}$ are Identity and zero matrices and x is as defined in (5). Constraints on the variations given in

(6),(7) can be rearranged into following matrix form.

$$\underbrace{\begin{bmatrix} q^T & 0_{1 \times 3} \\ -\omega^T q^\times & q^T \end{bmatrix}}_{\triangleq C} x = \begin{bmatrix} 0 \\ 0 \end{bmatrix}. \quad (11)$$

Remark: 1. Note that (10) and (11) constitute a constrained linear time-varying system. Furthermore, as noted in [14, Lemma 1], the constraint space is time-invariant, i.e., $Cx(0) = 0 \implies Cx(t) = 0, \forall t \geq 0$. Note that, unlike in [14], we obtained the variation-based linearization (8)-(9) by taking variations about the current state \mathcal{X} and not a desired state.

D. Variational Integrators

Conventional numerical integrators for the nonlinear dynamics in (2), do not ensure that the unit length of the vector q and the total energy are preserved numerically [9]. In this section, we present the variational integrator for spherical pendulum, to ensure that the dynamics evolve on S^2 . Discrete variational dynamics with time-step h for a spherical pendulum are given in [9] and are reproduced below,

$$q_{k+1} = \left(h\omega_k - \frac{h^2}{2m}(q_k \times mgle_3) \right) \times q_k + \left(1 - \left\| h\omega_k - \frac{h^2}{2m}(q_k \times mgle_3) \right\|^2 \right)^{1/2} q_k, \quad (12)$$

$$\omega_{k+1} = \omega_k - \frac{h}{2m}(q_k \times mgle_3) - \frac{h}{2m}(q_{k+1} \times mgle_3). \quad (13)$$

Let these equations be represented as,

$$\mathcal{X}_{k+1} = \int_{VI} f(\mathcal{X}_k). \quad (14)$$

E. Variations between two states on S^2

In Section II-B, we defined variation on S^2 . Thus, varying a pendulum state $\mathcal{X}_1 \in TS^2$ would result in a new state $\mathcal{X}_2 \in TS^2$ and let $x \in \mathbb{R}^6$ be the variation between these states. Furthermore, we can define operators to transform between them as follows. Consider $\ominus : TS^2 \times TS^2 \rightarrow \mathbb{R}^6$ and $\oplus : TS^2 \times \mathbb{R}^6 \rightarrow TS^2$ defined by

$$\mathcal{X}_2 \ominus \mathcal{X}_1 = x \quad \text{and} \quad \mathcal{X}_1 \oplus x = \mathcal{X}_2. \quad (15)$$

The mathematical formulae for the operators \ominus, \oplus are presented in Appendices A & B.

In the next section, we present the variation based extended Kalman filter (V-EKF) for spherical pendulum. Discrete variational dynamics in (14) are used in the *time* update to propagate the estimated state through time, while the Linearized dynamics in (10) are used to update the covariance of the estimated state.

III. VARIATION-BASED EXTENDED KALMAN FILTER

Given a linear dynamical system and a measurement model, with known Gaussian noise, the Kalman filter generates an optimal estimate of the state and its covariance. Kalman filters typically consist of two steps: (i) A *time* update, where the prior knowledge of the state along with the system dynamics are used to estimate the state at a later

time, and (ii) A *measurement* update, during which the estimate of the state and its covariance is updated based on the measurements received. An EKF is used for state estimation of nonlinear systems and measurement models by linearizing the dynamics and measurements.

Similarly, our proposed V-EKF uses the linearized dynamics and discrete variational dynamics presented in the previous section to estimate the state. V-EKF calculates the variation state between the pendulum states at time t_{k-1} and t_k , obtained by using discrete variational dynamics. This variation state is updated with the measurement at t_k . However, the estimated variation is not guaranteed to satisfy the constraint (11) and requires an additional constraint update. The estimated variation state and its covariance is projected onto the constraint surface. Finally, the variation state estimate is used to obtain the state estimate at t_k . Further details are provided in the subsequent subsections.

Notation followed by the V-EKF in this work is presented below.

A. Notation

- Let the estimates be represented by $\hat{\cdot}$, i.e., $\hat{\mathcal{X}}_k$ represents the pendulum state estimate at time t_k and \hat{x}_k represents the variation state estimate between the pendulum states $\hat{\mathcal{X}}_{k-1}$ and $\hat{\mathcal{X}}_k$.
- Let $\hat{\mathcal{X}}_k^-$ be *time* update of the pendulum state, \hat{x}_k^- be *time* update of the variation state and P_k^- be *time* update of the covariance of the variation state at time-step k .
- Let \hat{x}_k^m and P_k^m be the *measurement* updated variation state and the corresponding covariance.
- Let \hat{x}_k^+ and P_k^+ be the variation state and its covariance after the *constraint* update. Finally, let $\hat{\mathcal{X}}_k^+$ be the final pendulum state update.

In the following section, equations used by the variation based extended Kalman filter for state estimation are presented and the same is illustrated in the Figure 2.

B. Variation Based Extended Kalman Filter

1) *Time Update:* The equations of motions for spherical pendulum given in (2) along with gaussian process noise is represented as,

$$\dot{\mathcal{X}} = f(\mathcal{X}) + \mathcal{V}, \quad (16)$$

where \mathcal{V} is the process noise in the system. Since, the dynamics evolve on S^2 , the process noise $\mathcal{V} \notin \mathbb{R}^6$ but belongs to the tangent space of S^2 . Based on earlier result in (10), the variation-based linearization of the above dynamics results in

$$\dot{x} := \begin{bmatrix} \dot{\xi} \\ \delta\dot{\omega} \end{bmatrix} = Ax + v, \quad (17)$$

and the process noise of the variation state is $v \in \mathbb{R}^6$ with covariance $Q = \mathbb{E}[vv^T] \in \mathbb{R}^{6 \times 6}$. For practical applications, Q can be considered a design parameter.

Let the mean of the initial state of the spherical pendulum be $\hat{\mathcal{X}}_0$ and let the initial covariance of the variation state be $P_0 \in \mathbb{R}^{6 \times 6}$. The current *time* estimate $\hat{\mathcal{X}}_k^-$ is obtained by intergrating the dynamics in (16) using the variational

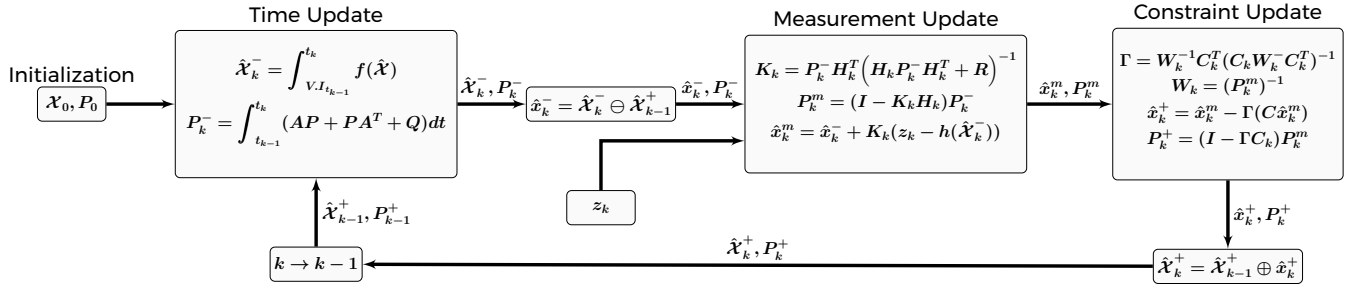


Fig. 2: Variation based extended Kalman filter illustrating the *time* update, *measurement* update and the *constraint* update.

integrator in (12)-(13) with the previous state estimate $\hat{\mathcal{X}}_{k-1}^+$ as initial condition. This is formulated as

$$\hat{\mathcal{X}}_k^- = \int_{V_I} f(\hat{\mathcal{X}}_{k-1}^+). \quad (18)$$

Next, the variation between the states $\hat{\mathcal{X}}_{k-1}^+$ and $\hat{\mathcal{X}}_k^-$ is calculated as explained in Section II-E, resulting in,

$$\hat{x}_k^- = \hat{\mathcal{X}}_k^- \ominus \hat{\mathcal{X}}_{k-1}^+. \quad (19)$$

Rest of the estimation is performed on the variation \hat{x}_k^- , effectively transforming the estimation from TS^2 to \mathbb{R}^6 . Covariance of the variation state is updated using the continuous covariance update given below (see [15, (3.235)]),

$$\dot{P} = AP + PA^T + Q, \quad (20)$$

where, A is the linearized dynamics from (10). Integrating this from t_{k-1} to t_k results in the *time* update of the covariance, P_k^- .

2) *Measurement Update*: The measurement $z \in \mathbb{R}^p$ is a nonlinear function of the state, as given below,

$$z = h(\mathcal{X}) + w, \quad (21)$$

where $w \in \mathbb{R}^p$ is Gaussian measurement noise with covariance $R = \mathbb{E}[ww^T] \in \mathbb{R}^{p \times p}$. Similar to an EKF [15], the above measurement model is linearized resulting in

$$z = Hx, \quad (22)$$

where $H \in \mathbb{R}^{p \times 6}$ is the measurement matrix (see Appendix-C for more details.). The *time* updated variation state \hat{x}_k^- and covariance P_k^- is fused with the measurement z_k at time t_k to obtain \hat{x}_k^m, P_k^m using the following measurement update:

$$\hat{x}_k^m = \hat{x}_k^- + K_k(z - h(\hat{x}_k^-)), \quad (23)$$

$$P_k^m = (I - K_k H_k) P_k^-, \quad (24)$$

where the Kalman gain $K_k = P_k^- H_k^T (H_k P_k^- H_k^T + R_k)^{-1}$.

3) *Constraint Update*: The variation state and its covariance \hat{x}_k^m, P_k^m obtained from the measurement update are not guaranteed to satisfy the constraint (11). We therefore need to project the estimates onto the constraint surface. This is achieved by projecting the estimates into the Null-space of the constraint matrix C , as explained in [7], [11]. The constraint update is thus given by,

$$\hat{x}_k^+ = \hat{x}_k^m - \Gamma(C\hat{x}_k^m), \quad (25)$$

$$P_k^+ = (I - \Gamma C_k) P_k^m, \quad (26)$$

where, $\Gamma = W_k^{-1} C_k^T (C_k W_k^{-1} C_k^T)^{-1}$ with W_k being a positive definite symmetric weight matrix. We choose $W_k = (P_k^m)^{-1}$ to obtain the smallest projected covariance [7].

Finally, the variation state estimate \hat{x}_k^+ is used to calculate the pendulum state estimate \mathcal{X}_k^+ as explained in Appendix-B

i.e.,

$$\hat{\mathcal{X}}_k^+ = \hat{\mathcal{X}}_{k-1}^+ \oplus \hat{x}_k^+. \quad (27)$$

An overview of the variation based extended Kalman filter (V-EKF) is illustrated in the Algorithm 1 and Figure 2.

Remark: 2. Note that the proposed V-EKF can also be extended to the case of an actuated spherical pendulum. In this case, the control input is used to propagate the state through the system dynamics, i.e.,

$$\dot{\mathcal{X}}_k^- = \int f(\hat{\mathcal{X}}_{k-1}^+, u_{k-1}), \quad (28)$$

with the rest of the estimation as in Algorithm 1.

Remark: 3. Note that the V-EKF can also be used to estimate states on other manifolds such as $SO(3)$ and $SE(3)$, and requires computing the variations on the respective manifolds.

IV. NUMERICAL SIMULATIONS

In this section, we demonstrate the variation based extended Kalman filter, proposed in the previous section, through numerical simulations. The measurement model is given by the position measurements of the pendulum mass with Gaussian noise. We implement the V-EKF to estimate the un-measured states and also obtain better estimates of the noisy measurements from sensors, while ensuring that the estimated states belong to TS^2 .

For numerical simulations of the spherical pendulum system, we use the following system parameters,

$$m = 1kg, \quad l = 1m.$$

We choose the noise statistics as follows: The initial covariance of the variation state is chosen as $P_0 = I_{6 \times 6}$, the measurement noise covariance is chosen as $R = 1e^{-3} I_{3 \times 3}$, and the process noise is $Q = 1e^{-5} I_{6 \times 6}$. The mean of the initial variation state is $\hat{x}_0 = 0_{6 \times 1}$, while the initial state of the pendulum is,

$$\hat{\mathcal{X}}_0 = [1, 0, 0, 0, 0, 0]^T.$$

Figure 3, illustrates the result of simulating the system with the V-EKF for 100 random initial conditions with the aforementioned measurement model and covariances. As seen from the Figure, V-EKF estimates of the state are close to the true state even with random initial states. More importantly, even with almost maximum initial attitude error, the estimates from the V-EKF still converge to the true values. In these simulations, measurements are obtained by running the dynamics simulation of the spherical pendulum with initial state $\hat{\mathcal{X}}_0$ and adding random process and measurement noises with covariances Q and R , respectively.

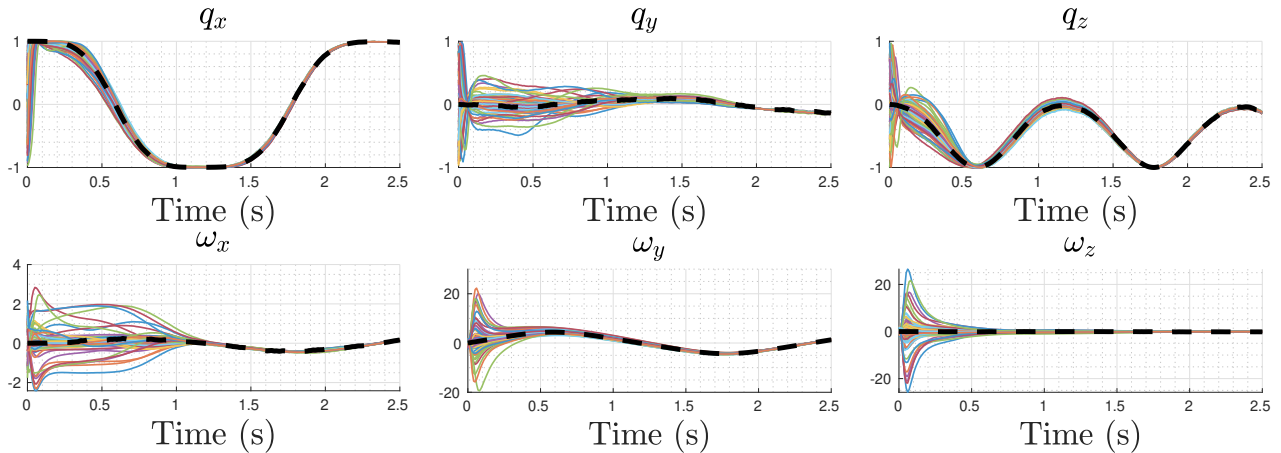


Fig. 3: *Convergence of V-EKF*: V-EKF was run 100 times with different random initial states, while using the same measurements, noise covariances and initial covariance. Noisy measurements are taken by simulating the spherical pendulum dynamics (with process noise). Figure shows convergence of the pendulum attitude (top row) and the angular velocity (bottom row) estimates and the dashed black line shows the true state.

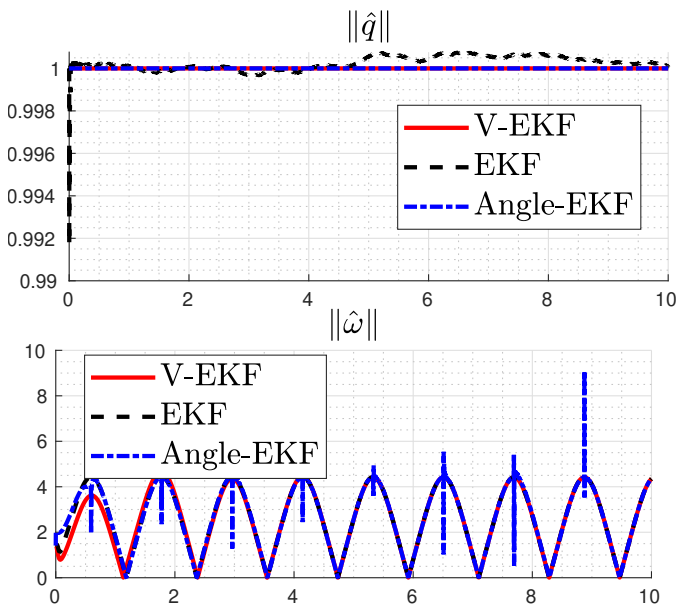


Fig. 4: Comparison between V-EKF, EKF (standard EKF applied on the dynamics in (2) through Jacobian linearization) and Angle-EKF (EKF applied on the dynamics represented using spherical coordinates); (Top) Plots for the norm of the load attitude estimate. (Bottom) Plot showing the norm of the estimated angular velocity.

Random initial conditions are selected by generating random variations with covariance P_0 and transforming the initial condition \hat{x}_0 through these variations (see Appendix-B).

Furthermore, the pendulum state estimated by the V-EKF lies on S^2 .i.e, the unit norm of the pendulum attitude is preserved and is shown in the Figure 4. In the Figure, norm of the pendulum attitude obtained through the V-EKF estimate is compared to that of a standard EKF (where the dynamics of the pendulum in (2) are linearized using Jacobians without taking variations on S^2 into consideration) and an angle-EKF (the dynamics of the pendulum are presented in the spherical

coordinates). Angle-EKF satisfies the unit-norm constraint, since the state q is as a function \sin and \cos of the angles. However, this representation results in singularities in the system and can be observed from the $\|\hat{\omega}\|$ plots in the Figure. This results in very high values for the angular velocity norm near the regions of singularities.

In order for the estimated variations to be valid, the variation estimates should also satisfy the constraint in (11). Figure 5 shows the constraint values during different stages of the estimation, namely (i) *time* update, (ii) *measurement* update and (iii) *constraint* update. As shown in the Figure, constraint projection update ensures that the variation estimate satisfies the constraint in (11). As seen from the Figures 3, 4, 5, the variation based extended Kalman filter is validated using numerical examples. In the next section, V-EKF is validated through experiments.

V. EXPERIMENTS

In this section, we present experimental results for the V-EKF developed in the previous sections. The physical setup used in the experiments as well as the results are discussed next.

A. Setup

The spherical pendulum model used for experiments consists of a 3D-printed cube, used as the pendulum bob, suspended from a fixed point through a string. Figure 6 shows the spherical pendulum used in the experiments. An Optitrack motion capture system and reflective markers on the pendulum bob and the cable suspension point are used to measure the relative position of the pendulum bob. System properties of the experimental setup are,

$$m = 0.0580 \text{ kg}, \quad l = 0.6665 \text{ m}. \quad (29)$$

An experiment is conducted by manually moving the pendulum bob to an initial attitude and letting go to have the spherical pendulum freely swing. The V-EKF is used to

Algorithm 1 *Variation Based Extended Kalman Filter*

System model and measurement model

$$\dot{\mathcal{X}} = f(\mathcal{X}) + \mathcal{V}$$

$$\dot{x} = Ax + v$$

$$z_k = h(\mathcal{X}_k) + w_k$$

$\mathcal{X}(0) \sim (\bar{\mathcal{X}}_0, \mathcal{P}_0)$, $x \sim (0, P_0)$, $v \sim (0, Q)$, $w \sim (0, R)$ where $f(X)$ and A are given in (16), (10).

Assumptions

$\{v(t) \text{ \& } w(t)\}$ are white noise processes uncorrelated with $\mathcal{X}(0)$ and with each other

Initialization

$$P_0^+ = P_0, \hat{\mathcal{X}}_0^+ = \bar{\mathcal{X}}_0$$

Prior (Time) update

- 1: *A priori* state update by integrating the dynamics using discrete variational dynamics given in (12), (13).

$$\hat{\mathcal{X}}_k^- = \int_{V.I. \cdot t_{k-1}}^{t_k} f(\hat{\mathcal{X}}_{k-1}^+) dt$$

- 2: Variation between $\hat{\mathcal{X}}_{k-1}^+$, $\hat{\mathcal{X}}_k^-$ is calculated (see Appendix-A).

$$\hat{x}_k^- = \hat{\mathcal{X}}_k^- \ominus \hat{\mathcal{X}}_{k-1}^+$$

- 3: Covariance update of the variation is obtained through integrating (20).

$$P_k^- = \int_{t_{k-1}}^{t_k} AP + PA^T + Q dt$$

Measurement update

- 1: Kalman gain is calculated using the *a priori* covariance and the measurement matrix H_k (see Appendix-C).

$$K_k = P_k^- H_k^T [H_k P_k^- H_k^T + R_k]^{-1}$$

- 2: Measurement update of the variation using the Kalman gain and measurement z .

$$\hat{x}_k^m = \hat{x}_k^- + K_k(z - h(\hat{x}_k^-))$$

- 3: Corresponding covariance update of the variation.

$$P_k^m = (I - K_k H_k) P_k^-$$

Constraint update

- 1: Constraint update by projecting the variation estimate into the constraint space,

$$\hat{x}_k^+ = \hat{x}_k^- - \Gamma(C\hat{x}_k^m)$$

- 2: Similarly, projecting the Covariance to lie in the constraint space.

$$P_k^+ = (I - \Gamma C_k) P_k^m$$

$$\Gamma = W_k^{-1} C_k^T (C_k W_k^{-1} C_k^T)^{-1}$$

$$W_k = (P_k^-)^{-1}$$

- 3: *A posteriori* state estimate is calculated using the updated variation (see Appendix-B).

$$\hat{\mathcal{X}}_k^+ = \hat{\mathcal{X}}_{k-1}^+ \oplus \hat{x}_k^+$$

estimate the state of the spherical pendulum using only the position measurements of the pendulum bob.

B. Results

To validate the proposed estimation through V-EKF, we show the estimated states of the pendulum and compare the results with the sensor measurements and standard EKF. Following noise statistics for the process model and mea-

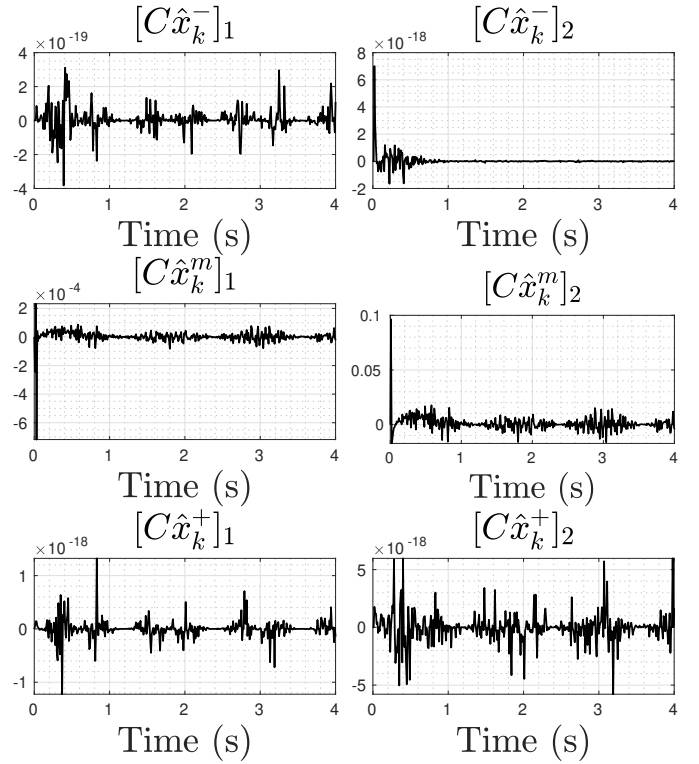


Fig. 5: *Constraint on various variation estimates*: The two columns illustrates the two constraints in (11). Constraint equation is valid for prior update (*first row*), however the measurement update (*second row*) does not satisfy the constraint equation. Finally, the constraint equation is satisfied after the constraint projection update (*third row*).

surement model are considered,

$$Q = \text{diag}([1, 1, 1, 100, 100, 100])e^{-5},$$

$$R = \text{diag}([1, 1, 1])e^{-3}.$$

Initial position of the pendulum-mass is measured for over a period of 10 seconds and the measured data is used to calculate the mean of the initial state and initial covariance of the variation state. Calculated $\bar{\mathcal{X}}_0$ and P_0 for the experiments are,

$$\bar{\mathcal{X}}_0 = [0.0070, 0.4017, -0.9157, 0, 0, 0]^T,$$

$$P_0 = \text{diag}([0.25, 5e^{-4}, 1e^{-4}, 3.49, 1e^{-2}, 1e^{-3}]).$$

Figure 7 shows the experiment results for state estimation of the spherical pendulum. Comparison between the V-EKF estimation, EKF estimation and the measurements is illustrated in the Figure. As shown in the Figure, V-EKF and EKF have similar estimates. However, advantage of V-EKF can be seen in Figure 8, which shows the plots for norm of q for various estimates. As seen from the Figure, norm of q is preserved only in the case of V-EKF. The offset in the case of the EKF estimate and the measurement can be attributed to the inaccurate measurement of the cable length. Such inaccuracies do not effect the structure of the state estimate for the V-EKF. Also shown in the plots for ω are the values of the angular velocity computed from finite differences of the measurement. The finite difference estimates are very noisy while the V-EKF estimates are smoother. Thus, as we have seen, variation based extended Kalman filter can be used to

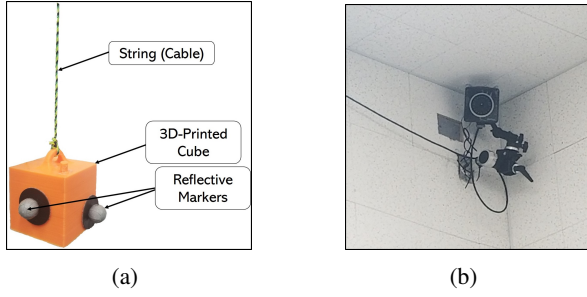


Fig. 6: Experimental setup for spherical pendulum model, a 3D-printed cube with reflective markers and a motion capture system to track center-of-mass position of the cube. (a) 3D-Printed cube with reflective markers suspended by a string, (b) Optitrack motion capture system estimate the states on S^2 .

VI. CONCLUSIONS

A variation based Extended Kalman Filter (V-EKF) is developed to estimate states of a spherical pendulum evolving on the two-sphere S^2 . Geometric variations on S^2 are used to obtain a variation-based linearization of the nonlinear geometric dynamics of the pendulum. The resulting linearized dynamics are time-varying with state constraints. The proposed V-EKF consists of a time update, a measurement update, and a constraint update, resulting in estimation of the states directly on TS^2 . Our method uses a coordinate-free formulation that is valid globally and is singularity-free. Numerical and experimental results are presented to validate the proposed V-EKF.

APPENDIX

A. Variation, x_k , between states \mathcal{X}_{k-1} and \mathcal{X}_k on S^2

($x_k = \mathcal{X}_k \ominus \mathcal{X}_{k-1}$):

The spherical pendulum attitude and angular velocity corresponding to the states \mathcal{X}_{k-1} and \mathcal{X}_k are given below,

$$\mathcal{X}_{k-1} = \begin{bmatrix} q_{k-1} \\ \omega_{k-1} \end{bmatrix}, \quad \mathcal{X}_k = \begin{bmatrix} q_k \\ \omega_k \end{bmatrix}. \quad (30)$$

In order to transform q_{k-1} to q_k while preserving the unit-length of q , we rotate q_{k-1} to q_k as shown in (3), where the rotation matrix is represented using exponential map ($\exp[\xi_k^\times]$), with $\|\xi_k\|$ equal to the amount of rotation and unit-vector along ξ_k representing the axis of rotation. The amount of rotation between q_{k-1} and q_k is given by the angle between the vectors q_{k-1} and q_k ,

$$\theta = \arccos [(q_{k-1} \cdot q_k)]. \quad (31)$$

Since q_{k-1} and q_k are unit-vectors, a vector perpendicular to the two unit vectors q_{k-1} , q_k is given by,

$$\vec{\xi}_k = \pm \frac{(q_{k-1} \times q_k)}{\|(q_{k-1} \times q_k)\|}. \quad (32)$$

Therefore, axis of rotation is found by finding the unit vector along $\vec{\xi}_k$ resulting in the least amount of rotation i.e.,

$$q_{(k)+} = \exp[(\theta \vec{\xi}_k)^\times] q_{k-1}, \quad (33)$$

$$q_{(k)-} = \exp[(-\theta \vec{\xi}_k)^\times] q_{k-1}, \quad (34)$$

$$\xi_k = \begin{cases} 0_{3 \times 1} & \text{if } \theta = 0, \\ -\theta \vec{\xi}_k & \text{else if} \\ \theta \vec{\xi}_k & \text{else.} \end{cases} \quad (35)$$

where, ξ_k is the infinitesimal variation between q_{k-1} and q_k .

The infinitesimal variation in the angular velocity, ($\delta\omega_k$), is similarly calculated using (3) as shown below. Taking time-derivative of (3) would result in,

$$\dot{q}_k = \exp[(\xi_k)^\times] (\dot{\xi}_k)^\times q_{k-1} + \exp[(\xi_k)^\times] \dot{q}_{k-1}. \quad (36)$$

Let $R = \exp[(\xi_k)^\times]$, therefore we have,

$$\dot{q}_k = R(\dot{\xi}_k)^\times q_{k-1} + R\dot{q}_{k-1}, \quad (37)$$

$$R^T \dot{q}_k - \dot{q}_{k-1} = -(q_{k-1})^\times \dot{\xi}_k, \quad (38)$$

since $a^\times b = a \times b = -b \times a = -b^\times a$, for any $a, b \in \mathbb{R}^3$.

From (10), we have, $\dot{\xi}_k = (q_{k-1} q_{k-1}^T (\omega_{k-1})^\times \xi_k + (I_{3 \times 3} - q_{k-1} q_{k-1}^T) \delta\omega_k)$ and substituting it in (38) results in,

$$R^T \dot{q}_k - \dot{q}_{k-1} = -(q_{k-1})^\times \left(q_{k-1} q_{k-1}^T (\omega_{k-1})^\times \xi_k + (I_{3 \times 3} - q_{k-1} q_{k-1}^T) \delta\omega_k \right).$$

Note $a^\times a a^T = 0_{3 \times 3}$, for any $a \in \mathbb{R}^3$. Therefore, (39) is simplified to,

$$R^T \dot{q}_k - \dot{q}_{k-1} = -(q_{k-1})^\times \delta\omega_k \quad (39)$$

$$(R^T \dot{q}_k - \dot{q}_{k-1})^\times (q_{k-1}) = - \left((q_{k-1} \cdot q_{k-1}) \delta\omega_k - (\delta\omega_k \cdot q_{k-1}) q_{k-1} \right)$$

Simplifying the above equation would result in,

$$\delta\omega_k = -(R^T \dot{q}_k - \dot{q}_{k-1})^\times (q_{k-1}) + (\delta\omega_k \cdot q_{k-1}) q_{k-1}. \quad (40)$$

From (6), we have $q \cdot \delta\omega_k = -(\xi_k^\times q) \cdot \omega$. This results in,

$$\delta\omega_k = -(R^T \dot{q}_k - \dot{q}_{k-1})^\times (q_{k-1}) - (\omega_{k-1} \cdot (\xi_k^\times q_{k-1})) q_{k-1}. \quad (41)$$

Also note that $\dot{q} = \omega \times q$ from (2). Finally, variation between

\mathcal{X}_{k-1} and \mathcal{X}_k is given by (35) and (41), i.e., $x_k = \begin{bmatrix} \xi_k \\ \delta\omega_k \end{bmatrix}$.

B. Calculating the state \mathcal{X}_k by transforming a state \mathcal{X}_{k-1} through a variation x_k ($\mathcal{X}_k = \mathcal{X}_{k-1} \oplus x_k$):

Variation x_k and state \mathcal{X}_{k-1} are decomposed as,

$$x_k = \begin{bmatrix} \xi_k \\ \delta\omega_k \end{bmatrix}, \quad \mathcal{X}_{k-1} = \begin{bmatrix} q_{k-1} \\ \omega_{k-1} \end{bmatrix}. \quad (42)$$

The transformed q can be calculated similar to (3) as follows,

$$q_k = \exp[(\xi_{k-1})^\times] q_{k-1}, \quad (43)$$

and the updated angular velocity is calculated using (39) as shown below,

$$\dot{q}_{k-1} = \omega_{k-1} \times q_{k-1}, \quad (44)$$

$$\dot{q}_k = R_2(\dot{q}_{k-1} - (q_{k-1})^\times \delta\omega_k), \quad (45)$$

$$\omega_k = q_k \times \dot{q}_k, \quad (46)$$

where $R_2 = \exp[(\xi_k)^\times]$. Therefore, perturbed state is given as,

$$\mathcal{X}_k = \begin{bmatrix} q_k \\ \omega_k \end{bmatrix}. \quad (47)$$

C. Linearization of measurement model to calculate measurement matrix H_k :

Position measurements are considered during the measurement update of the V-EKF. Measurement model is function

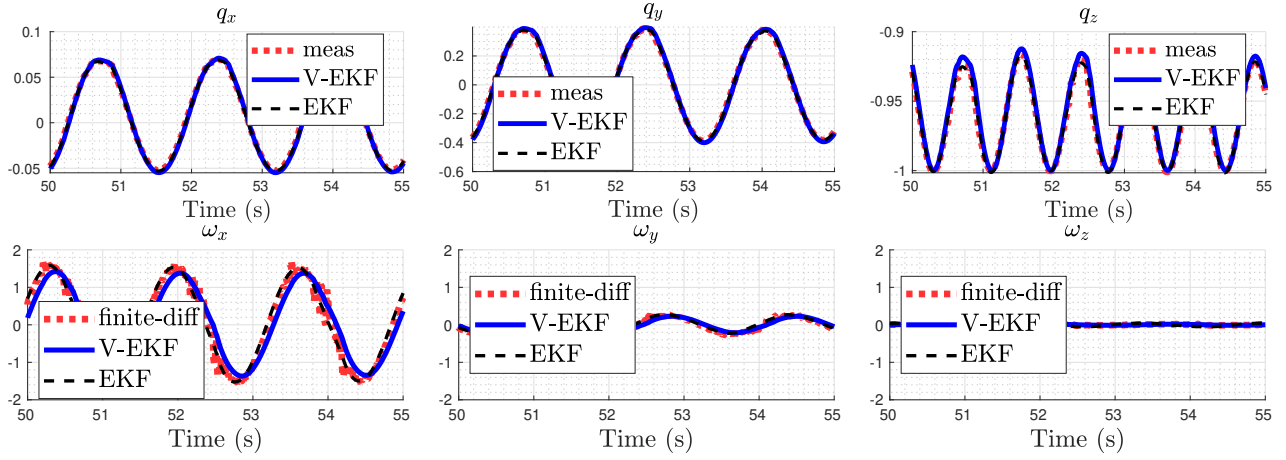


Fig. 7: Comparison between the experiment results obtained through V-EKF estimation (*solid line*), EKF estimation (*dashed line*) and the measurements (for \hat{q})/finite difference calculations (for $\hat{\omega}$) (*dotted line*). Top row shows load attitude estimate and angular velocities are shown in bottom row.

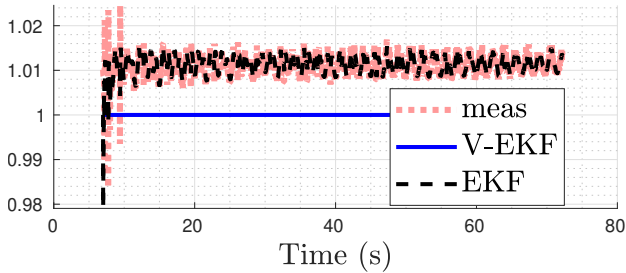


Fig. 8: Plots of the norm of load attitude obtained through (i). measurements (dotted line), (ii). V-EKF (solid line) and (iii). EKF (dashed line). Inaccurate measurement of the length of the spherical pendulum cable resulted in the offset in the norm for measurements and EKF. Also, note that the norm of q is preserved only in V-EKF estimation.

of spherical pendulum state and is given as,

$$h(\mathcal{X}_k) = lq_k. \quad (48)$$

This can be expressed in terms of variation as follows,

$$h(\mathcal{X}_k) \equiv h(x_k, \mathcal{X}_{k-1}) = l \exp[(\xi_k)^\times] q_{k-1}. \quad (49)$$

Measurement matrix H_k is obtained by linearizing the above equation with respect to variation x_k and evaluating at a priori state estimate \hat{x}_k^- as shown below,

$$H_k = \left. \frac{\partial h}{\partial x} \right|_{x=\hat{x}_k^-} = \left. \frac{\partial \left(l \exp[(\xi)^\times] q_1 \right)}{\partial \begin{bmatrix} \xi \\ \delta\omega \end{bmatrix}} \right|_{x=\hat{x}_k^-} \quad (50)$$

$$\Rightarrow H_k = l \left[\left. \frac{\partial \left(\exp[(\xi)^\times] q_{k-1} \right)}{\partial \xi} \right|_{x=\hat{x}_k^-} \quad 0_{3 \times 3} \right] \quad (51)$$

Derivative of an exponential-map of a vector w.r.t. the vector, i.e., $\left. \frac{\partial \left(\exp[(\xi)^\times] q_{k-1} \right)}{\partial \xi} \right|_{x=\hat{x}_k^-}$, is given in [3] or can be calculated using a symbolic toolbox. Thus, the measurement matrix, H_k , is as given in (51).

REFERENCES

[1] B. Bittner and K. Sreenath, "Symbolic computation of dynamics on smooth manifolds," in *Workshop on Algorithmic Foundations of*

Robotics (WAFR), 2016.

[2] A. Faust, I. Palunko, P. Cruz, R. Fierro, and L. Tapia, "Aerial suspended cargo delivery through reinforcement learning," *Department of Computer Science, University of New Mexico, Tech. Rep.*, 2013.

[3] G. Gallego and A. Yezzi, "A compact formula for the derivative of a 3-d rotation in exponential coordinates," *Journal of Mathematical Imaging and Vision*, vol. 51, no. 3, pp. 378–384, 2015.

[4] F. A. Goodarzi, D. Lee, and T. Lee, "Geometric control of a quadrotor uav transporting a payload connected via flexible cable," *International Journal of Control, Automation and Systems*, vol. 13, no. 6, pp. 1486–1498, 2015.

[5] F. A. Goodarzi and T. Lee, "Global formulation of an extended kalman filter on $se(3)$ for geometric control of a quadrotor uav," *Journal of Intelligent & Robotic Systems*, vol. 88, no. 2-4, pp. 395–413, 2017.

[6] E. Gregory and A. K. Sanyal, "A comparison study of state estimators for dynamics on the sphere," in *ASME 2012 5th Annual Dynamic Systems and Control Conference joint with the JSME 2012 11th Motion and Vibration Conference*. American Society of Mechanical Engineers, 2012, pp. 615–624.

[7] N. Gupta and R. Hauser, "Kalman filtering with equality and inequality state constraints," *arXiv preprint arXiv:0709.2791*, 2007.

[8] T. Lee, "Geometric control of quadrotor uavs transporting a cable-suspended rigid body," *IEEE Transactions on Control Systems Technology*, vol. 26, no. 1, pp. 255–264, 2018.

[9] T. Lee, M. Leok, and N. H. McClamroch, "Lagrangian mechanics and variational integrators on two-spheres," *International Journal for Numerical Methods in Engineering*, vol. 79, no. 9, pp. 1147–1174, 2009.

[10] —, "Stable manifolds of saddle equilibria for pendulum dynamics on s^2 and $so(3)$," in *Decision and Control and European Control Conference*, 2011, pp. 3915–3921.

[11] D. Simon and T. L. Chia, "Kalman filtering with state equality constraints," *IEEE transactions on Aerospace and Electronic Systems*, vol. 38, no. 1, pp. 128–136, 2002.

[12] K. Sreenath, T. Lee, and V. Kumar, "Geometric control and differential flatness of a quadrotor UAV with a cable-suspended load," in *IEEE Conference on Decision and Control (CDC)*, Florence, Italy, Dec. 2013, pp. 2269–2274.

[13] G. Wu and K. Sreenath, "Geometric control of quadrotors transporting a rigid-body load," in *IEEE Conference on Decision and Control*, Dec. 2014, pp. 6141–6148.

[14] —, "Variation-based linearization of nonlinear systems evolving on $SO(3)$ and S^2 ," *IEEE Access*, vol. 3, pp. 1592–1604, Sep. 2015.

[15] L. Xie, D. Popa, and F. L. Lewis, *Optimal and robust estimation: with an introduction to stochastic control theory*. CRC press, 2007.